Experimental and Theoretical Assessment of a Diesel Engine Using Different Palm Oil Methyl Ester (POME) Blends at Different Compression Ratios

Abhishek Samanta[1] · Prokash C. Roy[2]

Abstract In the variable compression ratio (VCR) diesel engine test setup, the palm oil methyl ester (biodiesel) was tested with diesel in varying quantities. The combustion and emission properties and the performance of diesel engines powered by biodiesel blends were examined and compared with conventional petroleum diesel. For combustion analysis, the engine's cylinder pressure profiles, mass fraction burned, start, and end of combustion while operating on various biodiesel blends under varying loads were acquired at CR 16, 17, and 18. B5 showed a higher quality of combustion in the cylinder pressure profile at zero load than B10, and as the load increased, the cylinder pressures for both B5 and B10 were nearly equal. Furthermore, it was discovered that brake thermal efficiency rises when load increases, but brake-specific fuel consumption falls. In the load range of 0–25% at compression ratio 18, B5 requires less brake-specific fuel than B10 and diesel. Compared to B10 and diesel, B5 exhibited the highest brake thermal efficiency at high loads at a compression ratio of 17. The emission of HC and CO was reduced at higher CR for B10 and B20, but the NOx formation was higher at higher CR.

Abbreviations

B10	Blend ratio of 90% diesel and 10% biodiesel
B15	Blend ratio of 85% diesel and 15% biodiesel
B20	Blend ratio of 80% diesel and 20% biodiesel consumptions
B5	Blend ratio of 95% diesel and 5% biodiesel
BTE	Brake thermal efficiency
CA	Crank angle
CD	Combustion duration
CI	Compression ignition
CO	Carbon monoxide
CP	Cylinder pressure
CR	Compression ratio
EBP	Ethanol blending programme
EOC	End of combustion
FFA	Free fatty acid
HC	Unburnt hydrocarbon
ID	Ignition delay
IEO	International energy outlook
ISFC	Indicated specific fuel consumptions
MFB	Mass fraction burned
MoPNG	Ministry of petroleum and natural gas
NDIR	Nondispersive infrared
NHR	Net heat release
NOx	Oxides of nitrogen
OECD	Organization for economic co-operation and development
POME	Palm oil methyl ester
SFC	Specific fuel consumption
SOC	Start of combustion
SOI	Start of Injection
TDC	Top dead center

✉ Prokash C. Roy
prokash.roy@gmail.com

1 Department of Automobile Engineering, Ranaghat Govt. Polytechnic, Ranaghat, Nadia 741201, West Bengal, India

2 Department of Mechanical Engineering, Jadavpur University, 188, Raja S.C. Mallick Rd, Kolkata 700032, India

1032

J. Inst. Eng. India Ser. C (October 2023) 104(5):1031–1046

Introduction

Advance economies require a spreading approach to energy, and satisfying recent climate changes are ambitious controversies in the modern era. The erratic fossil fuel price erodes energy security, and many governments support biofuel and biodiesel. Over the past few decades, significant dependency on the internal combustion engine (ICE) for the transport and energy generation sector has been observed. With an increase of 50% compared to the last 100 years, 60 million cars were produced globally only in 2012 [1]. Wherein 2019, the number had been increased to 67 million in car segments and only in India, the total engine operated vehicle production was about 5 million. ICE is used in the conventional approach for developing mechanical power against the chemical energy of fuel. Energy can be utilized from the resources of three categories, e.g., fissile, fossil, and renewable. The fundamental approach that described the durability & constancy of humanity's environmental, economic, and social aspects was termed 'sustainability' [2]. When abrupt transformation in the environment appears globally, it is unavoidable to explore renewable energy resources with sustainability. As claimed by IEO (International Energy Outlook)-2019, fossil-based petroleum energy consumption has been raised in Asia. In non-OECD countries, India, other parts in Asia & Africa, where the average growth rate was about 4% and population about two-thirds of the global population in 2018, energy utilization would rise by nearly 70% between 2018 and 2050 compared to a 15% rises in OECD regions. It had been forecasted that the oil reserves would be depleted within some decades if the consumption increased by 3% annually [3]. However, India's pace of rising energy demand is 6.5% per year, with imports covering 80% of the country's need for crude oil [4]. Hence energy security will be a significant factor in the near future.

The increase in energy utilization globally and nationally demands renewable resources for energy before the current conventional resources are crippled. In this context, biofuels have emerged, such as biodiesel. Biodiesel, specified as methyl ester, was substantial to nature and consisted of fatty acids. Biodiesel was formed from triglycerides by the approach of transesterification. It is an alternative renewable fuel that lessens the heavy reliance on petroleum diesel. Biodiesel also has enormous considerable accomplishments in the global climate. Biodiesel is sulfur-free, oxygenate, and biodegradable. Investigators observed that biodiesel reduces emissions, notably in the case of carbon monoxide, unburnt hydrocarbons, and soot emissions [5].

Amid different alternative renewable fuels, the acceptable fuel for the diesel engine is contemplated as biodiesel for better ignition quality, renewability, absence of aromatic and sulphur content, biodegradability with low greenhouse gas emission [6]. A diesel engine can be modified slightly or not at all to run on biodiesel. The qualities of biodiesel are also quite similar to those of diesel, but they have an oxygen content that is bonded to the fuel and have excellent miscibility with diesel without the use of a blending agent. Also, biodiesel has magnificent lubricity to lessen the wear and prolong the service life of the fuel injection pump [7].

Biodiesel in any percentage can be mixed with diesel for a biodiesel blend, and it enhances the mechanical efficiency of engines and cuts down the emissions of Sulphur oxides [8]. The high flashpoint of biodiesel improves operation safety and allows for direct application to diesel engines without significant modification [9]. Various car producers have recognized that biodiesel is an energy source adaptable to their diesel vehicles [10].

However, biodiesel also has particular deficiencies, like cold flow properties, inferior storage stability, and unsatisfactory spray characteristics with low heating value [11]. These deficiencies can be conquered with suitable feedstock for biodiesel and processing techniques.

The advancement of any nation is clinging to access to energy and resources. As a developing country, India requires a large scale of energy resources to sustain its rapid evolution. Fossil-based products like crude oil and coal are recognized among the main fossil resources for achieving energy requirements. In the near future, there will be a significant increase in the demand for fossil-based energy sources from the transportation industry, the agriculture and irrigation area, and small power plants.

In India, biofuel legislation could track the first biofuel legislation in 1948. Then the Parliament executed Act No. 22, Indian Power Alcohol Act, 1948. The Act's initial intention was to administer a fundamental approach to advancing the Indian 'power alcohol' production unit. However, Parliament had abolished the Act in the year 2000. The MoPNG finally provided the EBP in 2002, which required 5% ethanol blending in gasoline. However, because of the sugar molasses unavailability, uncontrolled ethanol pricing, technical setbacks by Government agencies, impeding delivery, and other factors, EBP proved ineffectual [12].

India now has the capacity to meet about 25% of the net demand for fossil fuels [13]. However, resources are imported to make up the shortfall, which uses a significant amount of the country's foreign currency. Therefore, improving convenient technology and renewable energy can be an assuring decision to the current ecological and energy difficulty [14]. Biodiesel importunity as 20% blending objective is predicted to increase by 19.8 L in 2020, whereas 31.1 billion liters in 2030. In India, the biodiesel generation primarily concentrated on *Jatropha* oilseed and other prospective tree-borne oils have to be examined effectively [15]. No single bio-source may satisfy the requirement of 20% blended fuel as outlined by India's biofuel strategy.

India's way of dealing with the biofuel program is described by a mix of reality and curiosity and the severe extent of aspiration inside them. It is novel because it did not depend on increasing or broadening traditional agriculture, regardless of whether for ethanol creation or biodiesel creation. On the other hand, various food grains like rapeseed, sugarcane, soybean, etc., are used by the USA, Brazil, and Germany. Furthermore, an unfavorable effect on edible oil accessibility may rise, which may increase food prices [16]. The creation of TBO for feedstock in barren land would prompt carbon sequestration and improve the biomass of the land. Palm can be chosen for the creation of biodiesel.

The largest producers of palm oil globally in the developing biodiesel sector are Asian countries like Malaysia and Indonesia (automobile & aviation) [17]. Oil palm conveys the greatest yield of vegetable oil from biomass in contrast to most crops [18] and at a cheap price relevant to alternative edible oils [19]. Palm oil methyl ester (POME) could be treated using fossil-based diesel. In 2014, the Malaysian government had authorized the enactment of B5 POME alongside petroleum diesel nationwide [20]. According to research published in 2018, industrial palm oil can produce enough biodiesel (POME) to adequately counterbalance Malaysia's entire diesel usage. On biodiesel consumption up to B7 in Malaysia, manufacturers offer engine guarantees. Without any significant modifications, the diesel engine can operate on biodiesel–diesel blends up to B100, which may offer a better environment in the future [21, 22]. 20% hydrocarbon emission and 13% CO (carbon monoxide) emission could be mitigated by the B20 biodiesel blend [23]. It was recognized that biodiesel leads to abrupt ignition delay preceding injection timing and excessive specific fuel consumption [24]. In combustion analysis at different compression ratios in a VCR engine, Nayak et al. [25] estimated that ignition delay for biodiesel strongly depends on injection pressure and atmospheric pressure. Lower compressibility and high viscosity resulted in less ignition delay.

To energize the creation of Biodiesel in India, the MoPNG declared a procurement policy of Biodiesel in October 2005 that got powerful from first January 2006. Under this approach, OMCs (Marketing companies in the Oil sector) are to buy Biodiesel (B 100), fulfilling the fuel quality guideline recommended by BIS for mixing with HSD (High-Speed Diesel) to the degree of 5% at distinguished buy habitats, the nation over. In January 2015, the Cabinet was chosen to permit the immediate offer of Biodiesel (B100) by private Biodiesel producers, their approved sellers and Joint Ventures of OMCs approved by MoPNG to all purchasers. The Government changed the High-Speed Diesel in August 2015 to allow a direct offer of Biodiesel (B100) to Bulk Consumers, such as Railways, State Road Transport Corporations, and other entities. On 10.08.2015, oil marketing companies in the country started selling blended biodiesel from a select few retail locations. Afterward, MoPNG gave notice on 29th June 2017 for changing the Motor Spirit and High-Speed Diesel, which expresses that the Central Government may allow the immediate offer of biodiesel (B100) for mixing with rapid diesel to all shoppers, subject to the conditions given. BIS revised IS: 1460 (Automotive Diesel Fuel Specification) in December 2017. Biodiesel adjusting to IS 15607 might be mixed up to 7 (% Vol) with car diesel fuel [26].

The Arecaceae, or palm family, includes the Elaeis guineensis (palm), a native tree to Africa that can reach heights of 20–30 m. In spite of this, it has been domesticated globally, including Malaysia, Sri Lanka, Indonesia, Thailand, Madagascar, Central America and West Indies [27]. Because they are a perennial tropical plant, palm trees do well in moist climates. Additionally, palm oil serves as the most popular feedstock for making top-promoted culinary oils and biodiesel. Less insecticides, water, and compost are needed for palm palms. [28]. For each acre of palm plantations, less daylight is needed. This biomass's production of 34% of the world's vegetable oil is substantial [29]. After 2 or 3 years of planting, the fruit of the palm tree is produced. The fruit may be collected for 25 years, and relative to other oilseed crops, more oil is produced per hectare. [30].

Commonly, CI engines are intended for diesel fuel. Utilizing diesel engines for biodiesel activity needs minor alterations in the engine working conditions. Researchers are recently showing more interest in simulating the engine performance to get optimum engine operating parameters instead of the build and test method. Also, engine makers consistently search for approaches to improve engine functions with reduced expenses and time-efficient development. Based on engine geometries, a single-zone combustion CI engine simulation model was developed [31]. To account for pressure fluctuations related to crank angle, engine power, and the mean effective pressure necessary for POME, a deviation in the specific heat ratio of the cylinder charge and burned gases was put into place [32]. Also, a simple model was introduced to predict the carbon monoxide and oxide nitrogen in combustion products in terms of mole fraction [33].

In the current work, palm oil biodiesel was produced using the transesterification approach. Then, B5, B10, B15, and B20 blends of palm oil biodiesel were examined using ASTM norms. In addition, an internal CI engine model was created to forecast the engine combustion nature and combustion products in terms of mole fraction for palm oil biodiesel blends (B5, B10). Finally, the combustion and emission parameter analysis were investigated along with engine performance for palm oil biodiesel blends compared with petroleum diesel at a variable compression ratio (CR 16, 17, and 18).

Biodiesel Production

With an alkali catalyst as opposed to an acid catalyst, transesterification proceeds very quickly. Catalyst potassium hydroxide was utilized to increase the biodiesel output and response rate. There are nine chambers in the trial setup. Five of them were important for palm oil biodiesel readiness. In the lower portion of Fig. 1, there were mixing chambers for the catalyst and methanol. These chambers were associated with a pump that helps siphon liquid to the main reactor. The primary reactor fan, which aided in mixing reactants, was present to speed up the rate of substance response. The desired temperature was maintained inside the chamber by temperature sensors and controls. For increased biodiesel production, temperature and time management were essential. Pumps and valves connected the main reactor to the glycerin column, where the product remained for some time. Due to different atomic weights, the upper segment was filled with biodiesel and the lower segment with glycerol. A valve at the bottom of the GC chamber opened, releasing glycerol. Biodiesel made up the remaining portion of the

Fig. 1 Actual view of the biodiesel production experiment setup

product, which was consumed subsequently. Biodiesel was not ready for use in engines.

It needed to be processed further. Continuous washing with water is required until the pH is estimated to reach 7. Methanol was used in excess to forward the reaction. After a thorough wash, biodiesel was heated for eight hours to 50 °C in a warmer broiler before being ready for use. The standard approach was used to inspect the significant fuel attributes for the produced POME blends (Table 1). Density was calculated using the fuel volume and mass. A viscometer (Redwood Model) was used to calculate the kinematic viscosity. The calorific value was calculated using a bomb calorimeter and the flashpoint was determined using a flashpoint analyzer (Silver Pensky-Martens, Model: VT4643).

Description of the Engine Setup

The local market was explored for refined palm oil. Biodiesel was created from palm oil via alkaline transesterification; the free fatty acid content was less than 0.61%. A single-cylinder, four-stroke, direct-injection, compression-ignition engine test setup has been used to investigate the combustion and performance characteristics of different blends as mentioned in Table 1. Table 2 contains the technical specifications as well as Fig. 2a represents the schematic for the experimental VCR (variable compression ratio). The engine was connected to a constant speed type eddy current dynamometer (Technomech Model TMEC10, 10BHP@1500–5000 RPM) that was operated by a computer interface (Apex Model AX-155). Cylinder pressure was measured using pressure sensor (Model S111A22). Through a data processing panel, the computer received and stored all of the instantaneous temperature and pressure using 'Engine soft' software. The software interface, created by Apex Innovation Pvt. Ltd., was used to collect the MFB results. Rassweiler and Withrow's method of burn rate analysis was used to estimate the mass fraction burned. [34]. The approach was based on the supposition that the pressure would rise per crank angle (Δp) during combustion. The pressure change during volume change (Δp_v) and the pressure rise during combustion (Δp_c) make up this pressure increase.
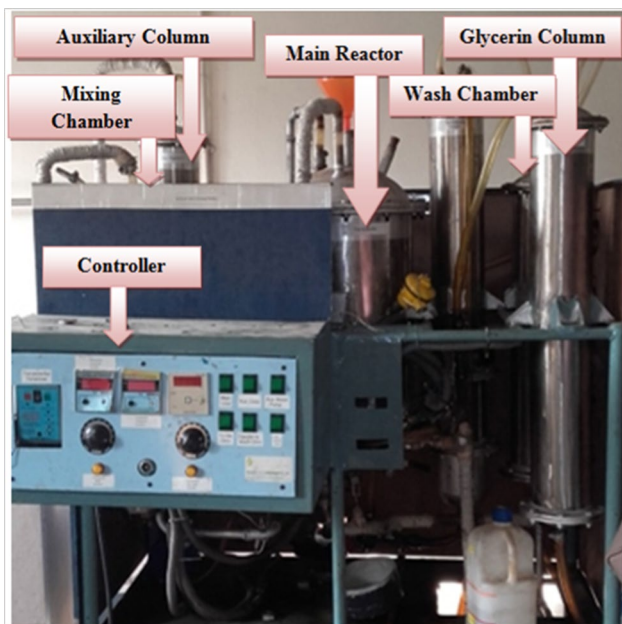
Table 1 Measured & standard value comparison of POME blends

Properties	Method	(B0)	B5	B10	B15	B20
Density (Kg/m^3)	–	832.6	833.2	848.6	856.3	865.9
Kinematic Viscosity (mm^2/s at 40 °C)	ASTM D2983	2.96	3.0	3.04	3.17	3.26
Flash Point (°C)	ASTM D93	68	74.6	77.3	78.1	79.5
Calorific Value (MJ/Kg)	ASTM D4809	45.9	44.5	43.3	41.6	40.7

Table 2 Technical specifications of experimental VCR engine

Parameter	Specification
Product	Computerized variable compression ignition engine
Type	Single cylinder, DI, diesel
Rated power	3.5 kW @ 1500 RPM
Compression ratio	12–18
Method of cooling	Water cooled
Injection timing	230 BTDC
Injection pressure	210 bar
Dynamometer	Eddy current, water cooled, with loading unit
Bore	87.50 (mm)
Stroke	110.00 (mm)
Swept volume	661.45 (cc)
Connecting rod length	234.00(mm)

$$\Delta p = \Delta p_c + \Delta p_v$$

A polytropic process could model pressure change cause of change in volume with an exponent k as,

$$p_{i+1} - p_i = \Delta p_c + p_i \left[\left(\frac{V_i}{V_{i+1}} \right)^k - 1 \right]$$

And $\Delta p_c = p_{i+1} - p_i \left(\frac{V_i}{V_{i+1}} \right)^k$

The MFB at the conclusion of the considered i-th interval may be estimated considering heat supplied to the in-cylinder was proportional to pressure rise, Δp_c as mentioned below.

$$MFB = \frac{m_b(i)}{m_b(\text{Total})} = \frac{\sum_0^i \Delta p_c}{\sum_0^N \Delta p_c}$$

where the combustion cycle had a start and stop at 0 and N, respectively. The engine tests were done at optimal constant speed of 1500 rpm with various loads (0%, 25%, 50%, 75%, & 100%). A compression ratio of 18:1, 17:1, and 16:1 was used for this study. Figure 2a and b show the Schematic Diagram and the real perspective of the engine arrangement, respectively.

Exhaust Emission Measurement Methods

The emission was measured using an Eco-Gas-100 Gas Analyzer by Manatec. Carbon monoxide concentration was measured in percent volume. The UHC and nitrogen oxides were measured in PPM. This gas analyzer for HC and CO used the NDIR technology detecting mechanism. The NOx sensor was used to measure nitrogen oxides. In Table 3, the technical specifications are listed.

Uncertainty Analysis

Uncertainty existed when gathering data from experimental instruments due to a number of operational and physical constraints. To confirm the accuracy of the experiment's precision and repeatability, an uncertainty analysis was conducted. An integrated analysis of uncertainty for the performance variables served as the guide for a thorough error evaluation. The analysis was conducted using the root mean square method, relying on $X1, X2,…, Xn$ to determine the uncertainty (ΔU) of a predicted outcome (Q) executing

Fig. 2 **a** Schematic engine test rig and **b** actual view of the experiment setup

1036

J. Inst. Eng. India Ser. C (October 2023) 104(5):1031–1046
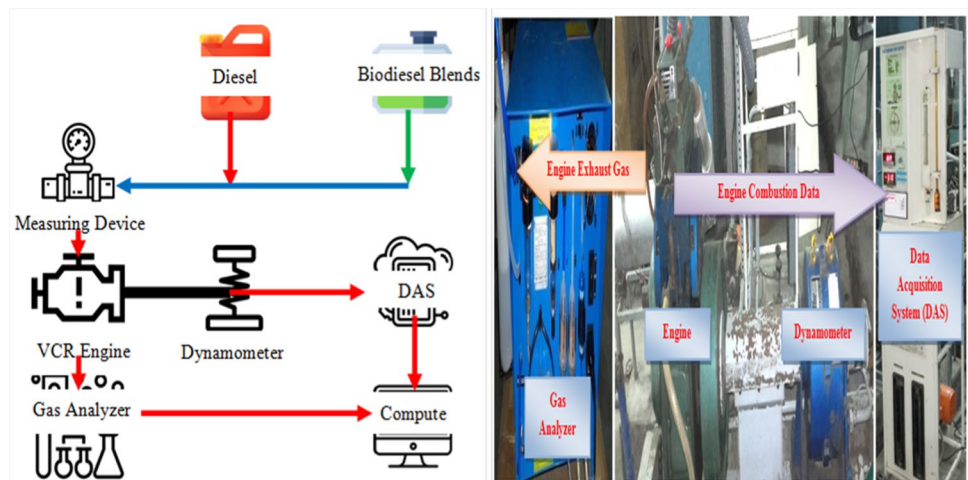
Table 3 Technical specifications of gas analyzer

Gas analyzer specifications	Make and model	Make Manatec, Model Eco Gas 100
	Technology & operating temperature	Non dispersive Infrared (NDIR) technology, +5–+45°C
Measurement parameters	CO (carbon monoxide)	Range: 0–15%, Resolution: 0.01%
	HC (hydro carbon)	Range: 0–20,000 PPM, Resolution: 1 PPM
	NOx (oxides of nitrogen)	Range: 0–5000 PPM, Resolution: 1 PPM

certain errors $\Delta X1, \Delta X2,\ldots, \Delta Xn$ of Eq. (1) [35]. The uncertainty was estimated in the calculated result based on the uncertainties in the primary measurements. Where result 'Q' is dependent factor of the $X1, X2,\ldots, Xn$.

$$\Delta U = \sqrt{\left(\frac{\partial Q}{\partial X_1}\Delta X_1\right)^2 + \left(\frac{\partial Q}{\partial X_2}\Delta X_2\right)^2 + \cdots + \left(\frac{\partial Q}{\partial X_n}\Delta X_n\right)^2} \tag{1}$$

The comprehensive uncertainty of the presented experimental results could be calculated as,

$$\text{Comprehensive Uncertainty} = \sqrt{\left(\text{Uncertainty}_{\text{BP}}\right)^2 + \left(\text{Uncertainty}_{\text{SFC}}\right)^2 + \left(\text{Uncertainty}_{\text{BTE}}\right)^2} = 2.63\%$$

Theoretical Considerations in Single Zone C.I Engine Model

A 4-stroke single zone thermodynamic model [36] had been established by taking into account several assumptions [31] together with the variation in specific heats against temperature [37]. Losses during heat release for fuel combustion were assumed to be lost via heat transfer [38]. To match actual diesel engine results, assumptions were made. Temperature, pressure, and equivalency ratio were the main factors influencing the ignition delay [39].

In the current study, it was considered that the combustion product contained just seven species ($CO, CO_2, H_2O, O_2, H_2, N_2, NO$). Combustion's chemical reaction could be expressed as,

$$C_xH_yO_1 + \frac{a}{\varphi} \cdot \left(O_2 + 3.76 \cdot N_2\right) \rightarrow n_1 \cdot CO + n_2 \cdot CO_2 + n_3 \cdot H_2O + n_4 \cdot O_2 + n_5 \cdot H_2 + n_6 \cdot N_2 + n_7 \cdot NO \tag{2}$$
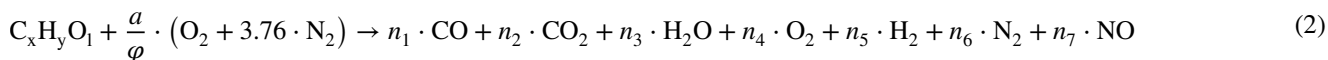
where, $\frac{a}{\varphi} = \frac{x + \frac{y}{4} - \frac{l}{2}}{\varphi}$

This reaction held true for mixtures that were lean, rich, and stoichiometrically balanced. It was supposed that neither carbon monoxide (CO) nor oxygen existed in the combustion product for the lean nor for the rich mixture, respectively. The value of $n_1, n_2, n_3, n_4, n_5, n_6, n_7$ indicates the number of moles of each individual product, while the value

of x, y, l, a indicates each individual reactant's mole number. Seven equations were necessary for Seven Unknowns ($n_1, n_2, n_3, n_4, n_5, n_6, n_7$) to be solved. Four equations were produced by the atoms of carbon, oxygen, hydrogen, and nitrogen being balanced.

The total mole fraction of all combustion products was taken into account to be 1.

The combustion had been taken into consideration for the CO_2, H_2O, CO, H_2 chemical equilibrium known as the water gas shift reaction.

$$CO + H_2O \Leftrightarrow CO_2 + H_2 \tag{3}$$

This reaction's equilibrium constant (k_p) was temperature-dependent and could alternatively be computed using the moles of the relevant species as follows:

$$k_p = \frac{n_2 \times n_5}{n_1 \times n_3} \tag{4}$$

The equilibrium constant's value are estimated using Gibbs function as below

$$k_p = \exp\left(-\frac{g^0_{CO_2}}{RT} - \frac{g^0_{H_2}}{RT} + \frac{g^0_{CO}}{RT} + \frac{g^0_{H_2O}}{RT}\right) \tag{5}$$

Also, considering the hypothetical equation,

$$\frac{1}{2}N_2 + \frac{1}{2}O_2 \Leftrightarrow NO \tag{6}$$

A family of seven substances is called NOx. About 80% of the air we breathe is made up of the comparatively harmless gas diatomic molecular nitrogen (N_2) However, the chemical element nitrogen (N) has ionisation levels (also known as valence states) that range from plus one to plus five and

is reactive as a single atom. So, there are numerous oxides that nitrogen can create. The three nitrogen oxides with the highest concentrations in the air are nitrous oxide (N_2O), NO, and NO_2. Primarily, NO is released as part of NOx emissions from combustion. When the combination is on the fuel-lean side of the stoichiometric ratio, combustion NO is created as a function of air to fuel ratio and is more evident [40]. Despite the fact that NO is quickly transformed to NO_2, only NO was considered an oxide of nitrogen in the current investigation to simplify modeling using Eq. (7) [1].

$$k_{NO} = \frac{n_7}{\sqrt{n_6} \times \sqrt{n_4}} \tag{7}$$

There were seven unknown values that were determined from those seven equations.

Results and Discussion

Combustion Chamber Pressure (CP)

Figure 3 shows how the chamber pressure varies with crank angle (CA) at different loads for POME blends (B5,

Fig. 3 Graphical illustration of the pressure versus CA (crank angle) using diesel (B0), POME blends (B5, B10, B15, B20) with CR 18:1 & CR 17:1 at different percent Loads (0, 25%, 50%, 75% and 100%)
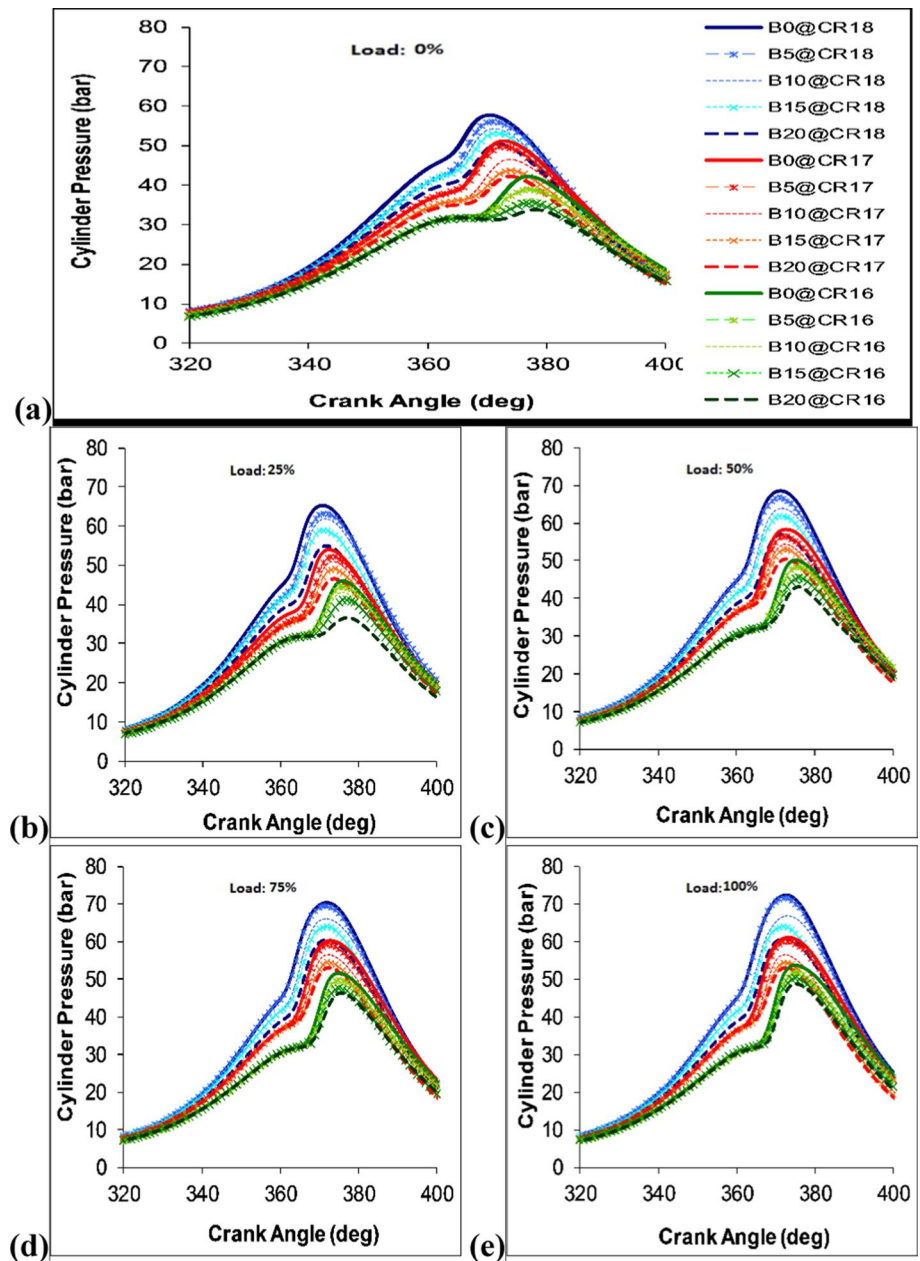
B10, B15, and B20) at CR 18, 17, and 16. All of the tested unique methyl ester mixtures (B5, B10, B 15, B 20) followed a chamber pressure pattern that was lower than that of diesel during the ignition period at five different engine load situations (0%, 25%, 50%, 75%, 100%). Furthermore, when the amount of biodiesel in blends increased, the peak pressure moved away from the TDC point. These phenomena resulted from biodiesel's poor atomization, instability, and decreased calorific value. The combustion chamber pressure of B5 methyl esters at various loads was lower but comparable to that of petroleum-based diesel at 75–100% load. However, other tried methyl ester blends' combustion pressure was considerably lower than petroleum-based diesel. Surprisingly, in chamber pressure during burning, B15 & B20 performed better at 75% to top load conditions at a compression ratio of 16:1. Due to additional fuel accumulating during the ignition delay period, the phenomena was caused by a rise in chamber temperature during mid- to top-load circumstances.

The effects of various compression ratios showed that, for petroleum base diesel and particular blends, max-CP consistently increased with compression ratio. The peak chamber pressure also migrated away from TDC with decreased CR. Because biodiesel mixes have higher densities than diesel, which causes a longer ignition delay, combustion starts later similar pattern experimented by Balamurugan et al. [41]. Compared to the other biodiesel blends, the combustion for B20 occurs at the furthest distance.

For CR 18, the peak CP was decreased by 20% when utilizing B20 compared with B0 and about a 3-degree CA delay. It might also be seen that B5 could compensate for this decrease in maximum pressure and longer ignition delay. Subsequently, it was noticed that the diesel fuel could be replaced by B5 fuel with a minimum amount of peak pressure loss. Bringing down the CR from 18 to 16 prompts a decrease in top CP from 72.29 to 53.68 bar (25%) for diesel and from 69.29 to 47.38 bar (31%) for B5, 64.74 to 46.58 bar (28%) for B10, 61.89 to 46.24 bar (25%) for B15, and 58.80 to 45.03 bar (23%) for B20 biodiesel blend at peak engine load condition. The results demonstrated that peak CP for all test fuels improved with a rise in CR, with the effect of CR being more significant in the B5 biodiesel blend than in petroleum diesel. Lower CR prompted lower gas temperature and, therefore, longer ignition delay. Consequently, the Maximum CP moves further from TDC, showing an increment in ignition delay.

The peak cylinder pressure at zero load conditions developed after TDC are shown in Fig. 4. Findings were contrasted with those from experiments using test fuels, B5, B10 and petroleum diesel. The comparison shows a thorough comprehension of the experimental results. The
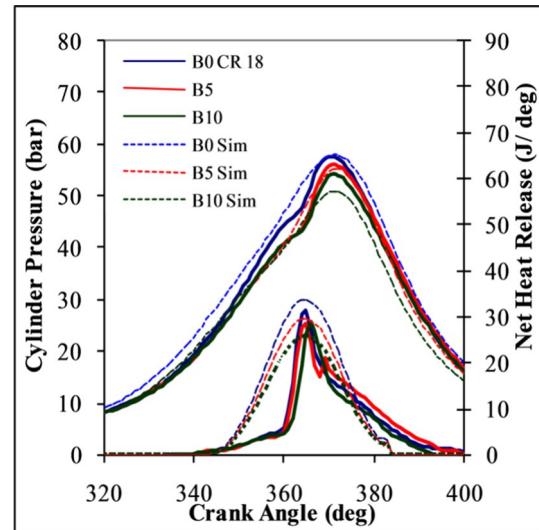
Fig. 4 Comparison of simulation and experimental cylinder pressure and NHR results

specific heat ratio significantly impacted the NHR models' accuracy for CI engines. The actual engine's cylinder temperature, dependent on flame speed and other combustion-related factors, determines the specific heat ratio. In this model, NHR was estimated using the single-zone model [1]. The simplification did not take into account flame speed. This could be the cause of the NHR simulation's variance from the experimental data's NHR during the initial stages of combustion.

Ignition Delay (ID)

The change of start of combustion (SOC) for diesel and several biodiesel blends (B5, B10, B15, & B20) is shown in Fig. 5. The SOC at each load was found to decrease with an increase in blending percentage. However, for some test fuels, the SOC increased as the engine load increased. Ignition delay indicates the period between the beginning of fuel injection and the beginning of combustion, which often occurs before the TDC. If the combustion process begins earlier than the expected TDC crank angle, the ignition delay stage is shorter since the fuel injection occurs at a constant CA. An increase in engine load shortens the ignition delay. This event was a direct result of the increased engine load, which increased the chamber's internal temperature and quickened the ignition of the fuel–air mixture. Additionally, it was found that the SOC dropped with the reduction in compression ratio, increasing ignition delay. Lower gas temperature was caused by lower CR, which led to a longer ignition delay.
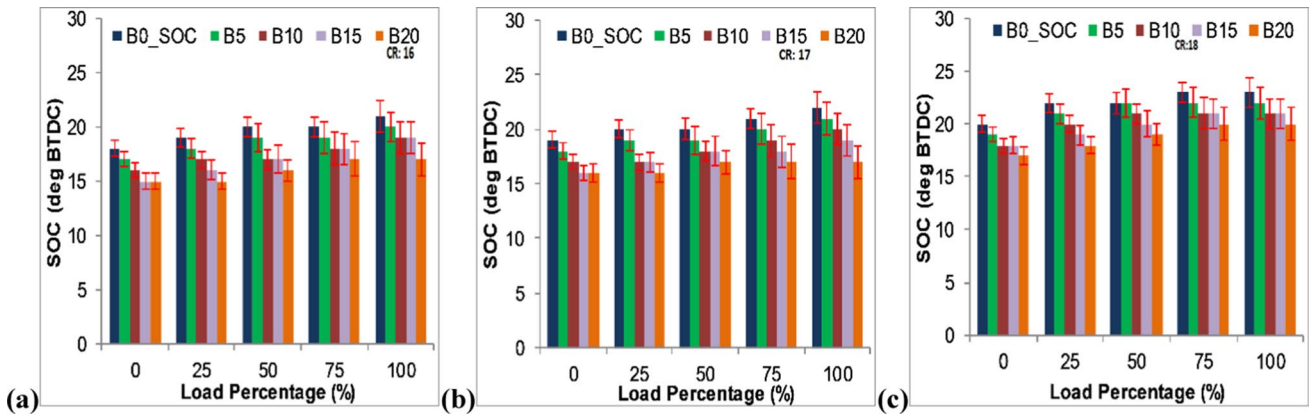
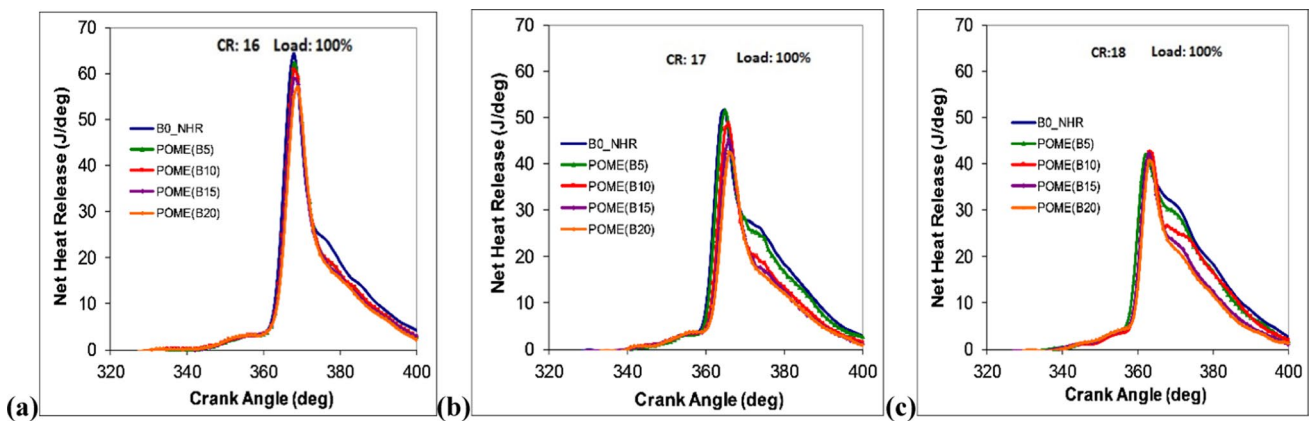**Fig. 5** Start of combustion at different loading condition (**a** CR 16, **b** CR 17, **c** CR 18)

Fig. 6 NHR versus CA variation using diesel (B0), POME blends (B5, B10, B15 & B20) (**a** CR 16, **b** CR 17 and **c** CR 18) at 100% load

Net Heat Release (NHR)

The change in the net heat release (NHR) is shown in Fig. 6 for different POME blends at CR 18, CR 16, with 100% engine load. The maximum NHR discrepancies were noted to be present at CR 16. Whereas the peak NHR across test fuels was just slightly higher at CR 18. The SOC, ignition delay, fuel mass burnt in the premixed phase at separate CR, and variation in various fuel ignition rates were all factors that affected the NHR rate. The peak NHR was seen in the figures to be lower for all the biodiesel blends compared to petroleum-based diesel at CR 16 and 17. At higher CR and 100% engine load, the peak NHR differences among test fuels were marginal. A slight delay in top NHR & SOC with a reduction in CR was noticed for both petroleum-based diesel and biodiesel blends (B5, B10, B15 & B20). An increase in peak NHR, from 41.8 to 64.27 J/CA (53%) with a reduction in CR from 18 to 16, was seen for diesel. An increase in top NHR, from 40.49 to 56.88 J/CA (40%) with a change

in CR from 18 to 16, was observed on B20 activity at peak engine load conditions. This phenomenon happened cause of the accumulation of more fuel in the combustion chamber and longer ignition delay with lower in-chamber gas temperature. Based on engine activity with biodiesel blends in the current investigation, higher NHR than diesel was seen at CR 18, particularly at higher CR settings. This event demonstrated a quicker ignition rate, perhaps because of the oxygen particle present in biodiesel atoms. Reducing the CR from 18 to 16 prompted a reduction in the peak NHR. Likewise, this event could be because of high viscosity leading to poor atomization in biodiesel blends, at a lower compression ratio due to longer ignition delay and more fuel accumulated. It was the reason behind the peak NHR value at lower CR.

Combustion Duration (CD)

Figures 5 and 7 show the different types of the start of combustion (SOC) and end of combustion (EOC), from which combustion duration (CD) at various engine loads might
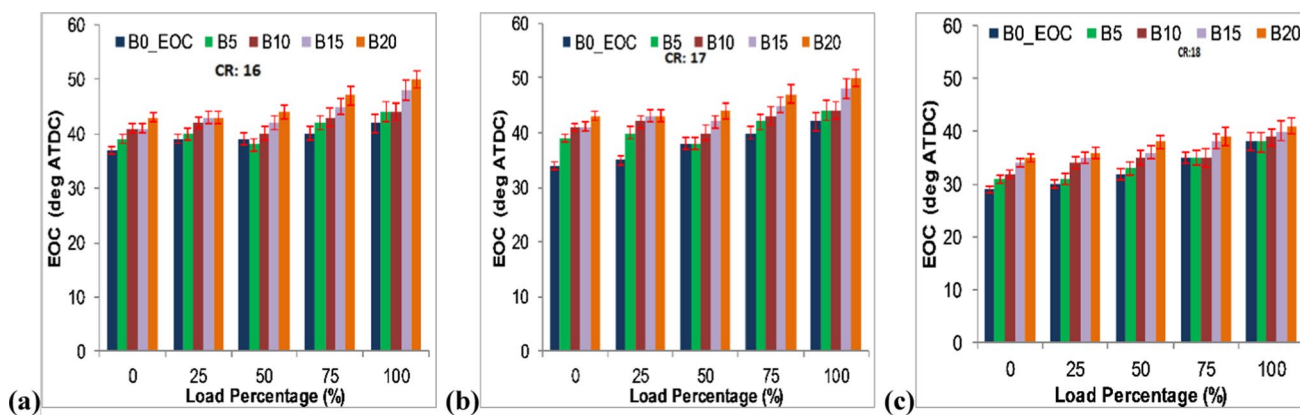
Fig. 7 Graphical illustration of the end of combustion at different loading condition (**a** CR 16, **b** CR 17, **c** CR 18)

be estimated. Between SOC and EOC is known as CD. The CA where there is an abrupt increase in heat release was selected as the SOC from the NHR curve. The cumulative heat release rate was used to calculate EOC. Using the data retrieval system's moving average for the probable heat release rate, the EOC value was determined. The EOC point might be thought of as the first time the average heat release rate fell below zero. When there is rapid burning with a delay in ignition, the combustion pressure and NHR rise quickly. When the NHR was raised from zero to a positive value, SOC was detected with regard to CA. From the graph, it can be observed that CD increased as engine loads increased for all biodiesel mixes and diesel. Due to more fuel being fed into the combustion chamber, this occurrence developed. A longer CD span results from boosting the biodiesel content of biodiesel blends. Higher fuel viscosity has an impact on atomization and vaporization, which has an impact on how well fuel mixes with air and how well sprays form. Because of its greater viscosity and surface tension, biodiesel has lower atomization quality [42] and requires more effort to burn. A lengthier CD was produced as a result of the sluggish combustion caused by this.

Mass Fraction Burned (MFB)

Variations of MFB with engine loads are shown in Fig. 8 for diesel and biodiesel blends. The MFB of the B5, B10, B15, and B20 blends showed a similar pattern to diesel. All tested biodiesel blends exhibited 5 and 10% MFB that appeared earlier than diesel at various engine loads. This occurrence was anticipated because all biodiesel blend fuel has a higher viscosity. The software interface called "Engine soft" by Apex Innovation Pvt. Ltd. was used to collect the MFB results. In diesel (B0), the 5 and 10% MFB amounts were considerably higher under all loading conditions than the B5 and B10 biodiesel blends. Due to the correct atomization of petroleum fuel, this phenomenon occurred. Additionally, it was noted that higher evaporation caused the value of 5 & 10% MFB to decline with increasing load. Based on the after-TDC (ATDC) crank angle, the 10% MFB was calculated and shown. According to experimental findings, the TDC point was nearly reached by blends of B5 and B10 when 10% of their mass fraction burned. Because of this,

Fig. 8 Graphical illustration of the mass fraction burned (**a** 5% MFB & **b** 10% MFB) at different loading condition (POME)
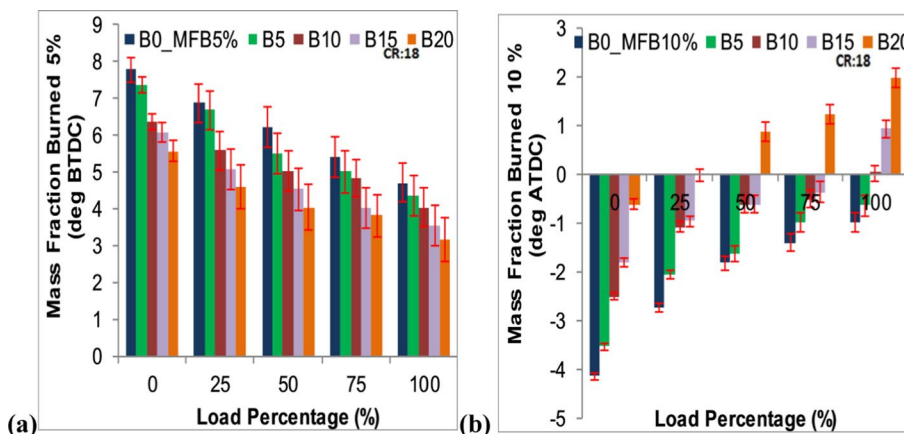
Fig. 9 a Brake thermal efficiency at different loading condition at CR 18. **b** Brake thermal efficiency at different CR (diesel & biodiesel blends)

(a)   (b)
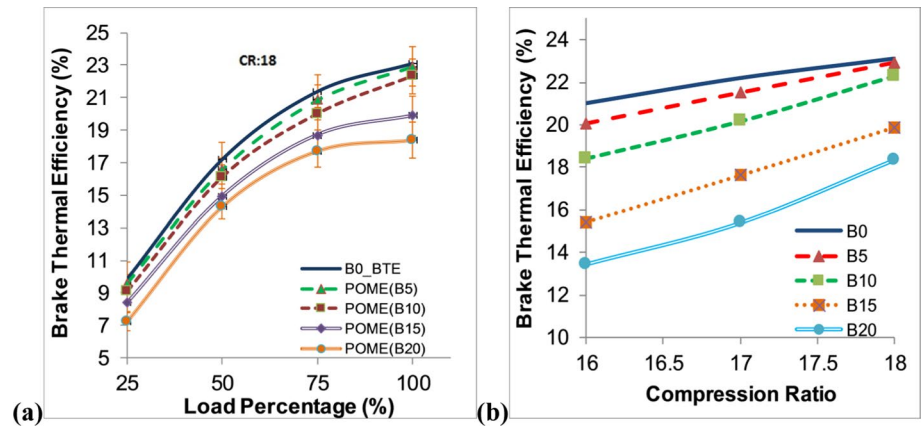
in Fig. 8's B5 & B10 blends, 10% of the MFB value was almost nonexistent.

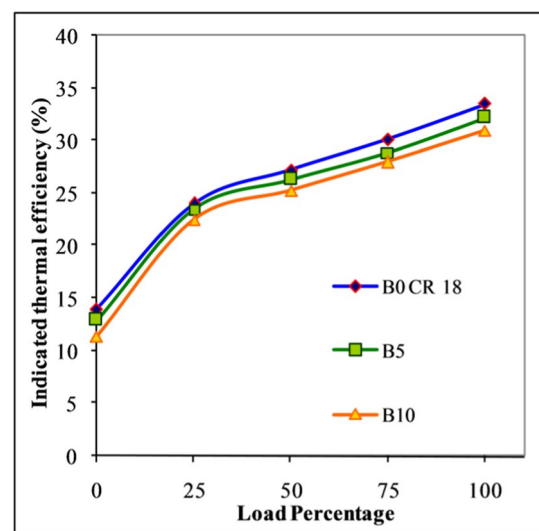### Brake Thermal Efficiency (BTE)

Figure 9 a shows that the brake thermal efficiency (BTE) of all the tested fuels tended to rise with an increase in engine load. In this analysis, the highest BTE for diesel was noted. Since diesel had a higher LHV and a suitable air–fuel ratio, the result was complete combustion. From the graph, it can be seen that B5 and B10 exhibit higher BTE at full engine load than B15 and B20. Because of the fuel's increased lubricity—possibly due to higher viscosity and sulphur content in the blends—this phenomenon was caused. Since B15 and B20 had higher densities and lower LHVs at full engine load than B5 and B10, their BTE was lower. BTE was shown to increase first due to the increase in load but then to decrease due to the subsequent increase in load. The more fuel burned as the engine load grew, the higher the BMEP. When this happened, the BTE initially increased. However, the BTE curve displayed a decreasing pattern after a 75% engine load. This phenomenon occurred because the combustion process took less time to complete as the load increased past 75% engine load at high temperature and BMEP, which resulted in a greater demand for fuel and an increase in energy consumption. As the amount of biodiesel in the fuel increased, it was observed that BTE decreased. Fuel LHV and viscosity were the factors that affected this aspect.

A lower heating value and hence less force were created as the biodiesel content increased, which resulted in a fall in BTE. Low BTE was caused by inadequate fuel injector atomization, low power output, and increased fuel viscosity with increased biodiesel concentration. The difference in BTE values between the various blends was caused by increased density and viscosity values. The test fuel loses vaporisation and atomization when it becomes too viscous and dense. Blends of biodiesel fuels burned unevenly due to

poor vaporisation and atomization. The increased viscosity and lower heating value of biodiesel cause poor atomization and poor preparation of fuel–air mixture during ignition delay, delaying the commencement of biodiesel combustion. The diesel BTE for diesel was at its highest in this examination. With the increase in biodiesel concentration came fuel viscosity, leading to poor fuel injector atomization, low power output, and low BTE. When operating the engine with diesel fuel and POME 20 (B20), Jamshaid et al., 2022 reported a similar result [43].

The variation of BTE for diesel, B5, B10, B15, and B20 blends at peak engine load are shown in Fig. 9b for CR 16, 17, and 18. It was observed that as the CR rose, the BTE did as well. This phenomenon was caused by the rise in BMEP that accompanied the rise in CR. Due to high CP and temperature, which ensured superior burning and resulted in high BTE, the BMEP increased with an increase in CR. The

Fig. 10 Graphical illustration of the simulated Indicated thermal efficiency at different loading condition

1042

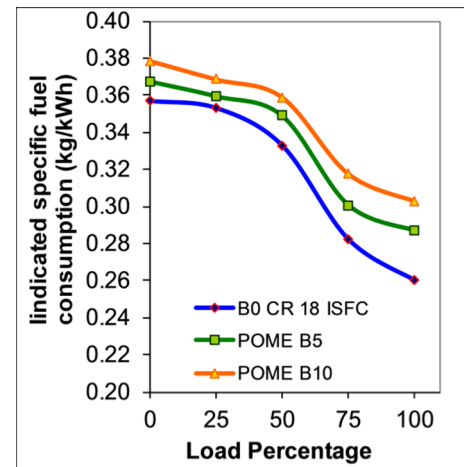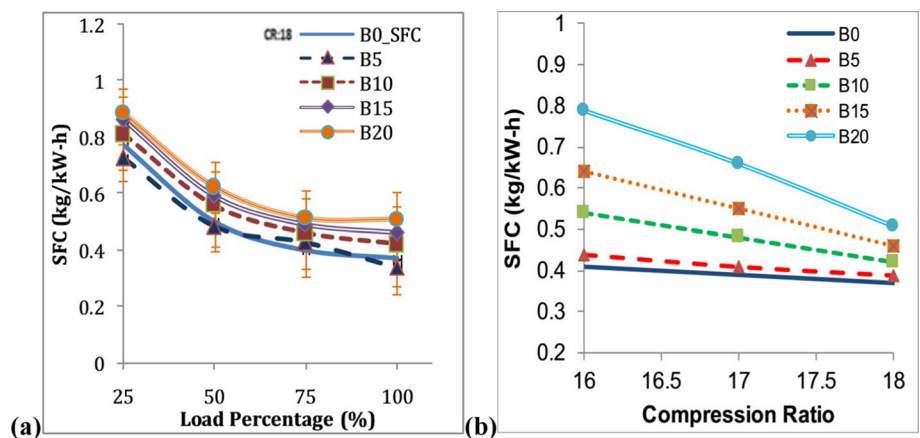J. Inst. Eng. India Ser. C (October 2023) 104(5):1031–1046

addition of more biodiesel largely resulted in a decrease in BTE. However, it was discovered that BTE for B5 and B10 was higher than that of petroleum-based diesel at CR 18:1. The high temperature caused this characteristic, and CP that formed in the chamber at CR 18:1, as well as the biodiesel's greater oxygen content. Diesel's maximum engine load resulted in the highest BTE, recorded at 23.12% (CR 18:1).

Figure 10 shows the simulated model's indicated thermal efficiency and the trend lined up with the direction of the actual engine's BTE. The variations in simulated ITE between B0, B5, and B10 under 0–25% engine loading conditions were found to be negligible. Additionally, there was a rapid increase in ITE, from 0 to 25% load state.

Specific Fuel Consumption (SFC)

The amount of fuel used to produce one power unit was defined as SFC. The same SFC trend was followed for all test fuels containing biodiesel, as shown in Fig. 11a. Diesel has a lower SFC at all engine loads than B5, B10, B15, and B20. The reason for the higher SFC was the higher density and lower LHV. For all of the test fuels between 0 and 50% load conditions, the SFC variations were negligible. B20 differed from the other test fuels in terms of SFC under peak load conditions. It was shown that test fuels with greater biodiesel content had higher SFCs. The fuel required to deliver a unit of power increased as the LHV fell with the biodiesel percentage, which increased the SFC values. The test fuel's density was another element that impacted SFC. The densities were observed to rise as the biodiesel content did. Since more fuel was injected for a given load, the fuel mass flow rate was raised. The increase in density would result in inadequate fuel injector atomization, resulting in less efficient burning and reduced power production. It was observed that the SFC values were dropping with the load. The B5, B10, B15, and B20 biodiesel blends followed the same pattern as petroleum-based fuel.

Fig. 12 Graphical illustration of the simulated Indicated SFC at different loading condition

However, the engine power output exceeded the fuel consumption, resulting in reduced SFC. The fuel utilization increased as the load increased. Figure 11b shows the SFC variations in CR up to 18:1 from CR 16:1. The diagram displays the range of SFC with CR at maximal engine load circumstances. The SFC values declined as the CR increased. This pattern was caused by the fact that BMEP grew as CR increased.

According to Fig. 12, which shows the indicated SFC from the simulated model, the trend closely matched the direction of the SFC for the real engine. Between 0 and 25% engine loading circumstances, it was noted that B0, B5, and B10 showed only slight variances in the simulated ISFC. Between 50 and 100% load circumstances, the ISFC also started to decline.
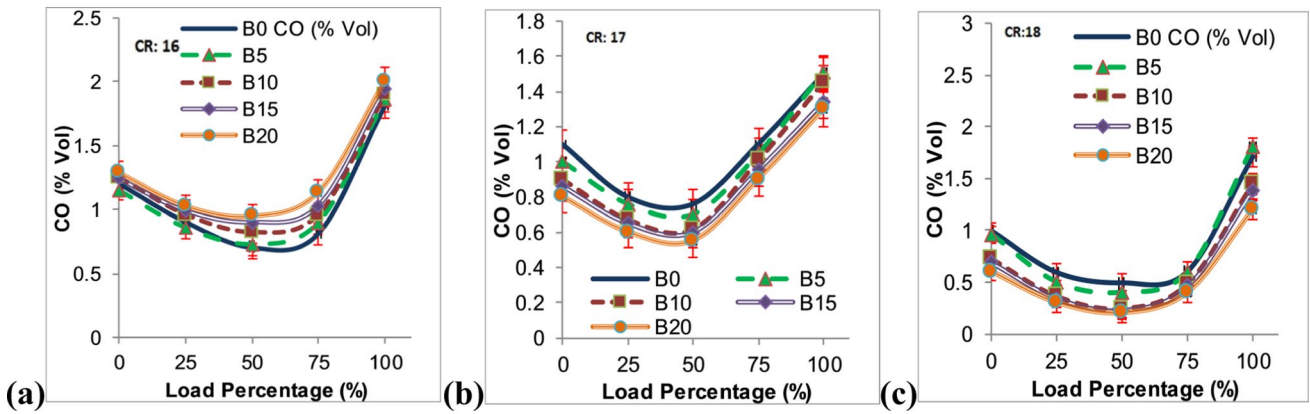
Fig. 11 **a** Specific fuel consumption at different loading condition (CR 18) **b** Specific fuel consumption (diesel & biodiesel blends) at different CR (16, 17 and 18)

Fig. 13 Graphical illustration of the carbon monoxide emission at different loading condition. (**a** CR 16, **b** CR 17 and **c** CR 18)

Emission (CO)

The CI engine emits little carbon monoxide because it typically operates at a low engine load and a lean fuel–air ratio. Due to insufficient air surrounding the fuel atoms or a lack of time to complete the combustion cycle, the fuel–air mixture failed to satisfy the combustion, resulting in a significant CO emission. The incomplete fuel combustion in the CI engine led to CO emissions. Figure 13 shows the fluctuation of CO emissions with engine load for all fuels tested. According to the graph, B20 had the lowest CO emission when compared to the other test fuels separately under various load circumstances, as more oxygen was present. The CO emissions first dropped up to 50% engine load before unexpectedly rising at increasing engine load. The leaner fuel–air mixture burned at 50% engine load and reduced CO emissions. The excessive fuel-to-air ratio caused more smoke to be produced and hindered the oxidation of CO to CO_2, which led to increased emissions. B20 fuel was shown to emit less CO than the other test fuels. When operating at maximum load with 17:1 CR, B20's CO emission was around 13% lower than diesel. The CO emission in B20 fuel activities was assessed with increasing CR (17:1–18:1). For instance, when the CR was raised from 17:1 to 18:1, the CO emanations in B20 gasoline reduced by nearly 23% at peak load.

Also, the impact of CR on CO emission has appeared in Fig. 13. The emission of CO exceptionally relies upon the burning temperature and accessibility of oxygen. A decrease in CR from 18 to 16 prompted an increase in CO emissions by 40% for B20, while it was observed higher emission of CO at B20 blend in CR to 16 compared to petroleum diesel. The reason was that more fuel accumulated at CR 16. Also, lower emission of CO was recorded under engine activity with CR settings 17:1 and 18:1. Biodiesel blends recorded lower CO emissions at CR 17 & 18 cause of oxygen present in the biodiesel structure.
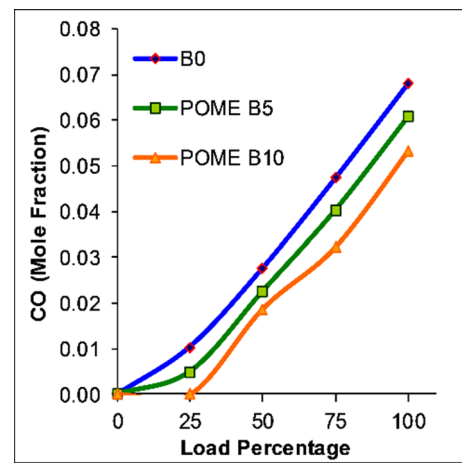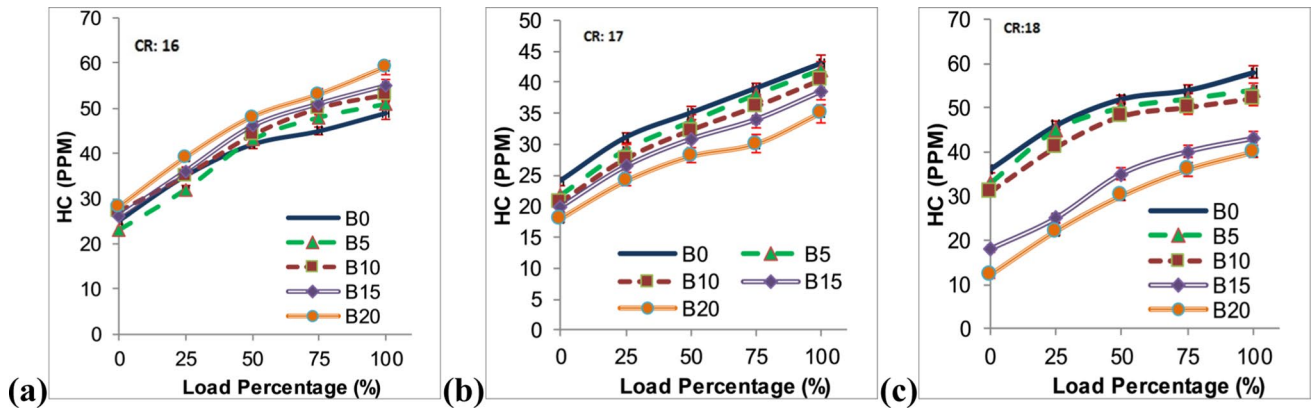

Fig. 14 Graphical illustration of the simulated carbon monoxide emission at different loading condition

The lean fuel–air mixture simulation model had no CO, and the rich mixture simulation model had no oxygen in the byproducts. The simulated mole fraction of CO emission is shown in Fig. 14. At a 25% load situation, the equivalence ratio was more significant for just diesel and the B5 POME blend, with a value of more than one (rich fuel–air combination). At the same time, it was less significant for the B10 POME blend (lean mixture). These ER readings came from experimental results. Because of this, at a 25% load situation, the CO mole fraction measurements of the B10 POME blend were nil.

Emission (HC)

Figure 15 portrays the variety of HC emissions with engine load for blends (B5, B10, B15, B20). The outcomes presented that the HC discharges incremented with expanding engine load. At 17 CR and zero engine load, the evaluated HC discharge was 25 ppm for diesel, but it increased to

Fig. 15 Graphical illustration of the unburnt hydrocarbon emission at different loading condition. (**a** CR 16, **b** CR 17 and **c** CR 18)
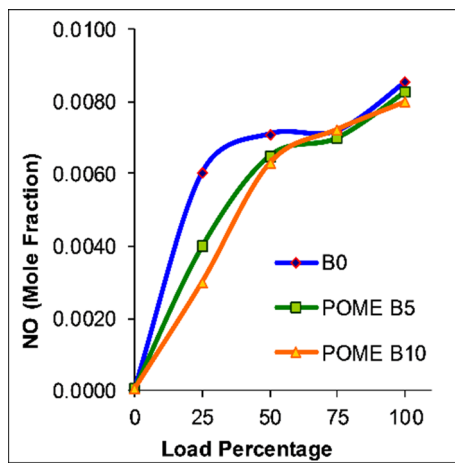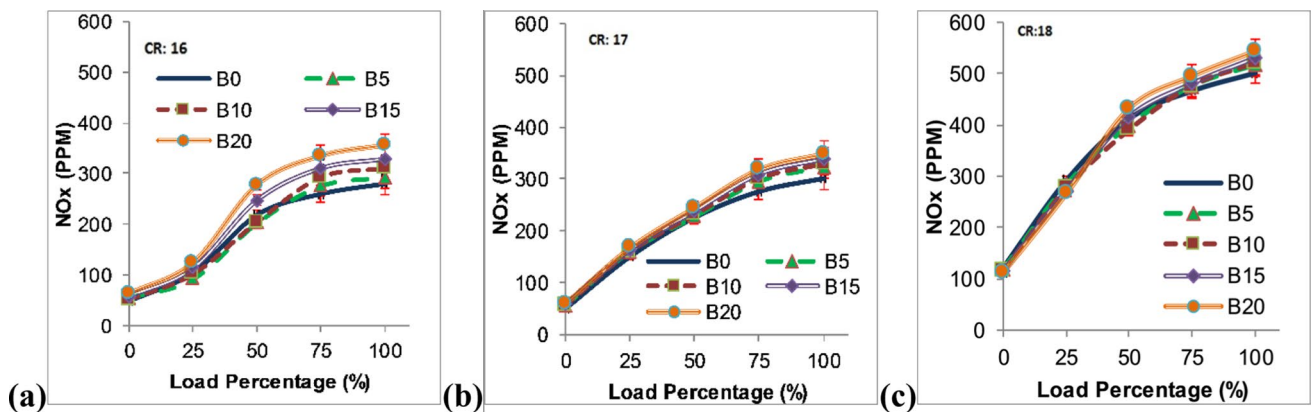

Fig. 16 Graphical illustration of the simulated oxides of nitrogen emission at different loading condition

43 ppm at peak engine load. However, at CR 16, the HC emission was marginally higher for biodiesel blends at peak load conditions caused by more fuel accumulation at

the ignition delay period. The expanded emission of HC at higher engine load was because of oxygen inadequacy; leaner fuel–air burning offers lower HC emissions. Like this, the HC emissions decreased with tested biodiesel blends at all engine loads as for diesel at CR (17:1 and 18:1). It had occurred cause of improved oxygen content in tested biodiesel blends, which prompted complete fuel burning. With expanding CR (17:1 to 18:1), HC's emission was reduced for B15 and B20 because higher CR offers high CP and temperature, which improves fuel burning.

Emission (NOx)

Figure 16 displays the simulated mole percentage of nitrogen oxides (NOx) emission as the combustion byproducts. However, the NOx mole fraction results for diesel and POME blends (B5 & B10) were not zero at zero load conditions. For NOx, the mole fractions were around 0.0007, 0.0005, and 0.0004, respectively. Additionally, the highest combustion temperature was considered while determining the equilibrium constant value for the generation of

Fig. 17 Graphical illustration of the oxides of nitrogen emission at different loading condition. (**a** CR 16, **b** CR 17 and **c** CR 18)

nitrogen oxides. The peak temperature for POME blends from the simulation results was lower than diesel. The simulated mole fraction values for NOx emission were shallow and close to zero; nevertheless, they were considerably higher during peak load conditions.

Figure 17 portrays the emission of NOx outcome of different engine loads at different CR. The emission of NOx was fundamentally made with dissociation of the climatic nitrogen at high adiabatic flame temperature conditions. It was strongly developed with maximum ignition temperature, oxygen presence, and NOx formation time. It was observed that at higher engine load, NOx increased with an increase in engine load. This event resulted from the considerable fuel consumed at a higher engine load, followed by high CP and temperature, and consequently, NOx increased. Also, the emission of NOx development was higher at CR 18 for all the tested biodiesel blends and diesel. This increased NOx discharge was because of the oxygen presence with biodiesel blends, specifically B20.

Conclusions

An assessment was conducted to evaluate the use of POME biodiesel blends (B5, B10, B15, and B20) compared to diesel (B0) from the perspectives of combustion, performance, and emission on an unaltered diesel engine. Tests were conducted to determine the sample biodiesel blends' viscosity, calorific value, density, and flash point. The results achieved were quite similar to petroleum diesel. The single-zone model was used to verify the precise results acquired from the standard diesel engine. The combustion nature had been accurately predicted by the thermodynamic model using B0, B5, and B10. However, a noticeable variation showed the impact of the model assumptions. A combustion product model predicted the mole per cent of CO and NO emissions from the engine. The simulated NO discharge was somewhat higher under top load conditions and slightly lower at low load situations. The CP and combustion chamber temperature rose at 18:1 CR, which caused an early SOC and decreased the NHR. BTE and SFC also improved at higher CR. HC and CO were reduced as the CR increased for B10 and B20. But the generation of NOx increased. Without any engine modifications, the engine could successfully run on biodiesel blends. The engine could run on biodiesel blends as high as B20. Because of the density and lower heating value, the engine could be operated at a BTE that was slightly lower than that of diesel. All the tested POME biodiesel blends had a BTE that was slightly lower than petroleum diesel. Higher density and viscosity values ultimately led to poor atomization, and as a result, lower BTE

was attained for the tested POME biodiesel blends. Additionally, the SFC was higher than it was for petroleum diesel due to higher viscosity values. As a result, higher SFC was seen in tested POME biodiesel blends. Four biodiesel blends—B5, B10, B15, and B20—were used to analyse the engine's combustion, performance, and exhaust. Compared to other biodiesel blends, B5 and B10 offered superior performance and fewer emissions. In light of this, it might be inferred that POME blends (B5, B10, B15, & B20) can be used successfully to power a diesel engine that hasn't been altered.

Declarations

Competing interests   The authors do not have any conflict of interest amongst themselves in submitting this article to this journal.

References

1. R.D. Reitz, Directions in internal combustion engine research. Combust. Flame **160**, 1–8 (2013). https://doi.org/10.1016/j.combustflame.2012.11.002

2. S. Das, D. Kashyap, P. Kalita, V. Kulkarni, Y. Itaya, Clean gaseous fuel application in diesel engine: a sustainable option for rural electrification in India. Renew. Sustain. Energy Rev. (2020). https://doi.org/10.1016/j.rser.2019.109485

3. Y.C. Sharma, B. Singh, Development of biodiesel: current scenario. Renew. Sustain. Energy Rev. **13**, 1646–1651 (2009)

4. M. Suresh, C.P. Jawahar, A. Richard, A review on biodiesel production, combustion, performance, and emission characteristics of non-edible oils in variable compression ratio diesel engine using biodiesel and its blends. Renew. Sustain. Energy Rev. **92**, 38–49 (2018)

5. W.N.M. Wan Ghazali, R. Mamat, H.H. Masjuki, G. Najafi, Effects of biodiesel from different feedstocks on engine performance and emissions: a review. Renew. Sustain. Energy Rev. **51**, 585–602 (2015)

6. S. Semwal, A.K. Arora, R. Badoni, D.K. Tuli, Biodiesel production using heterogeneous catalysts. Biores. Technol. **102**, 2151–2161 (2011)

7. P. Tamilselvan, N. Nallusamy, S. Rajkumar, A comprehensive review on performance, combustion and emission characteristics of biodiesel fuelled diesel engines. Renew. Sustain. Energy Rev. **79**, 1134–1159 (2017)

8. A.A. Kumar, Biofuels (alcohols and biodiesel) applications as fuels for internal combustion engines. Prog Energy Combust Sci. **33**, 233–271 (2007)

9. J. Singh, S. Gu, Commercialization potential of microalgae for biofuels production. Renew Sustain Energy Rev **14**, 2596–2610 (2010)

10. A.M. Ashraful, H.H. Masjuki, M.A. Kalam, I.M. Rizwanul Fattah, S. Imtenan, S.A. Shahir, H.M. Mobarak, Production and

comparison of fuel properties, engine performance, and emission characteristics of biodiesel from various non-edible vegetable oils: a review. Renew Sustain Energy Rev. **80**, 202–228 (2014)

11. R.D. Misra, M.S. Murthy, Blending of additives with biodiesels to improve the cold flow properties, combustion and emission performance in a compression ignition engine—a review. Renew Sustain Energy Rev **15**, 2413–2422 (2011)

12. P.K. Biswas, S. Pohit, What ails India's biodiesel programme? Energy Policy **52**, 789–796 (2013)

13. S. Dhar, P.R. Shukla, Low carbon scenarios for transport in India: co-benefits analysis. Energy Policy **81**, 186–198 (2015). https://doi.org/10.1016/j.enpol.2014.11.02

14. H. Singh Pali, A. Sharma, Y. Singh, N. Kumar, Sal biodiesel production using Indian abundant forest feedstock. Fuel (2020). https://doi.org/10.1016/j.fuel.2020.117781

15. N. Scarlat, J.-F. Dallemand, F. Monforti-Ferrario, M. Banja, V. Motola, Renewable energy policy framework and bioenergy contribution in the European union–an overview from national renewable energy action plans and progress reports. Renew. Sustain. Energy Rev. **51**, 969–985 (2015). https://doi.org/10.1016/j.rser.2015.06.062

16. S. Pohit, P.K. Biswas, R. Kumar, A. Goswami, Pricing model for biodiesel feedstock: a case study of Chhattisgarh in India. Energy Policy **38**, 7487–7496 (2010)

17. I. Mukherjee, B. Sovacool, Palm oil-based biofuels and sustainability in Southeast Asia: a review of Indonesia, Malaysia, and Thailand. Renew. Sustain. Energy Rev. **37**, 1–12 (2014)

18. M. Koushki, M. Nahidi, F. Cheraghali, Physico-chemical properties, fatty acid profile and nutrition in palm oil. J. Paramed. Sci. (2015). https://doi.org/10.22037/jps.v6i3.9772

19. B.M. Siddique, M.H. Ibrahim, S. Hena, Physicochemical properties of blends of palm oil with other vegetable oils. Grasas Aceites **61**, 423–429 (2010). https://doi.org/10.3989/gya.010710

20. H. Adnan, Palm oil biodiesel programme to cover all of Malaysia by July, The star online, https://www.thestar.com.my/business/business-news/2014/04/26/b5-goes-nationwide/ (2014)

21. A.G. Wahab, Malaysia biofuels annual, in *Service*, ed. by U.F.A USDA Foreign Agricultural Service (2016)

22. K.R. Szulczyk, A.R. Khan, The potential and environmental ramifications of palm biodiesel: evidence from Malaysia. J. Clean. Prod. (2018). https://doi.org/10.1016/j.jclepro.2018.08.241

23. A.M. Hupp, J. Perronb, N. Roquesb, J. Crandallb, S. Ramosc, B. Rohrbackc, Analysis of biodiesel-diesel blends using ultrafast gas chromatography (UFGC) and chemometric methods: extending ASTM D7798 to biodiesel. Fuel **231**, 264–270 (2018)

24. M. Canakci, J.H. VanGerpen, Comparison of engine performance and emissions for petroleum diesel fuel, yellow grease biodiesel, and soybean oil biodiesel. Trans. ASAE Am. Soc. Agric. Eng. **46**(4), 937–944 (2003)

25. S.K. Nayak, P.C. Mishra, S. Tripathy, Influence of compression ratio on combustion characteristics of a VCR engine using *Calophyllum inophyllum* biodiesel and diesel blends. J. Mech. Sci. Technol. **29**(9), 4047–4052 (2015). https://doi.org/10.1007/s12206-015-0850-2

26. N.P.B, National Policy on Biofuels, *Ministry of Petroleum and Natural Gas Notification,* (2018)

27. M.H. Jayed, H.H. Masjuki, M.A. Kalam, T.M.I. Mahlia, M. Husnawan, A.M. Liaquat, Prospects of dedicated biodiesel engine vehicles in Malaysia and Indonesia. Renew. Sustain. Energy Rev. **15**, 220–235 (2011)

28. T. Silalertruksa, S.H. Gheewala, P. Pongpat, P. Kaenchan, N. Permpool, N. Lecksiwilai, R. Mungkung, Environmental sustainability of oil palm cultivation in different regions of Thailand: greenhouse gases and water use impact. J. Clean. Prod. **167**, 1009–1019 (2017)

29. É.G. Castanheira, F. Freire, Environmental life cycle assessment of biodiesel produced with palm oil from Colombia. Int. J. Life Cycle Assess. **22**, 587–600 (2017)

30. A. Samanta, S. Goswami, P.C. Roy, Producing biodiesel and optimized by taguchi design against palm oil as sustainable alternative fuels in Bangladesh. Int. Energy J. **20**(3), 411–420 (2020)

31. A. Samanta, S. Kumar, P.C. Roy, Modeling and performance analysis of compression ignition engines using biodiesel as fuel, *International Journal of Scientific & Engineering Research*, vol 7(4), ISSN 2229-5518, (2016)

32. A. Samanta, P.C. Roy, An empirical investigation of biodiesel engine fuelled with palm oil methyl ester biodiesel blends. Int. J.Vehicle. Struct. Syst. **12**(1), 85–88 (2020). https://doi.org/10.4273/ijvss.12.1.19

33. A. Samanta, P.C. Roy, Pragmatic analysis on performance & emission and a single zone engine model development with inedible neem & waste vegetable oil biodiesel blend (B10). Int. J. Energy Clean Environ. **22**(1), 53–89 (2021)

34. J.B. Heywood, *Internal Combustion Engines Fundamentals* (McGraw Hill Publications, New York, 1988), pp.491–667

35. A. Paul, R. Panua, D. Debroy, An experimental study of combustion, performance, exergy and emission characteristics of a CI engine fueled by diesel-ethanol-biodiesel blends. Energy (2017). https://doi.org/10.1016/j.energy.2017.09.137

36. M. Yıldız, B. Albayrak Ceper, Zero-dimensional single zone engine modeling of an SI engine fuelled with methane and methane-hydrogen blend using single and double wiebe function: a comparative study. Int. J. Hydrog. energy (2017). https://doi.org/10.1016/j.ijhydene.2017.07.016

37. A. Sakhrieh, E. Abu-Nada, I. Al-Hinti, A. Al-Ghandoor, B. Akash, Computational thermodynamic analysis of compression ignition engine. Int. Commun. Heat Mass Transf. **37**, 299–303 (2010)

38. J.C. Lin, S.S. Hou, Performance analysis of an air-standard Miller cycle with considerations of heat loss as a percentage of fuel's energy, friction and variable specific heats of working fluid. Int. J. Therm. Sci. **47**, 182–191 (2008)

39. S. Richard, *Introduction to Internal Combustion Engines*, 2nd edn. (Society of Automotive Engineers Inc., Warrendale, PA, 1994)

40. Clean Air Technology Center (MD-12), Nitrogen Oxides (NOx), Why and How They Are Controlled, Clean Air Technology Center, EPA-456/F-99–006R, (1999)

41. T. Balamurugan, R. Nalini, Experimental investigation on performance, combustion and emission characteristics of four stroke diesel engine using diesel blended with alcohol as fuel. Energy **78**, 356–363 (2014)

42. R.K. Pandey, A. Rehman, R. Sarviya, Impact of alternative fuel properties on fuel spray behavior and atomization. Renew. Sustain. Energy Rev **16**, 1762–1778 (2012)

43. M. Jamshaid, H.H. Masjuki, M.A. Kalam, N.W.M. Zulkifli, A. Arslan, A.A. Qureshi, Experimental investigation of performance, emissions and tribological characteristics of B20 blend from cottonseed and palm oil biodiesels. Energy **239**, 121894 (2022). https://doi.org/10.1016/j.energy.2021.121